Implications of multi-modal age distributions in Pleistocene cave deposits: A case study of Maludong palaeoathropological locality, southern China

Darren Curnoe[a,*], Jian-xin Zhao[b], Maxime Aubert[c], Mian Fan[d], Yun Wu[d], Andy Baker[a], Goh Hsiao Mei[a], Xue-feng Sun[e], Raynold Mendoza[a], Lewis Adler[f], Shiwu Ma[g], Les Kinsey[h], Xueping Ji[d]

[a] ARC Centre of Excellence for Australian Biodiversity and Heritage, Palaeontology, Geobiology and Earth Archives Research Centre, School of Biological, Earth and Environmental Sciences, The University of New South Wales, Sydney, NSW 2052, Australia
[b] School of Earth and Environmental Sciences, University of Queensland, Brisbane, QLD 4072, Australia
[c] Griffith Centre for Social and Cultural Research and Australian Research Centre for Human Evolution, Griffith University, Gold Coast Campus, QLD 4222, Australia
[d] Yunnan Institute of Cultural Relics and Archaeology, Research Centre for Southeast Asian Archaeology, Kunming, Yunnan 650118, China
[e] School of Geography and Ocean Science, Nanjing University, Nanjing 210023, China
[f] Bioanalytical Mass Spectrometry Facility, Mark Wainwright Analytical Centre, The University of New South Wales Australia, Sydney, NSW 2052, Australia
[g] Mengzi Institute of Cultural Relics, Mengzi, Yunnan 661100, China
[h] Research School of Earth Sciences, Australian National University, Canberra, ACT 2600, Australia

ABSTRACT

The occurrence of multi-modal ages for inclusions contained within cave sediments is probably far more widespread and problematic than has been appreciated by archaeologists until now. This phenomenon is likely to be a relatively common situation in caves especially in tropical/sub-tropical areas like southern China where karstification and sedimentation would have been rapid within a context of active hydrological regimes over protracted periods during the Pleistocene. The availability of various cost-effective dating techniques applicable to both Pleistocene cave sediments and a range of sedimentary inclusions means that archaeologists are now better placed to understand this phenomenon than ever before. Here we describe the results of Uranium-series dating of a randomly selected sample of deer bones and teeth from Maludong in southern China which demonstrate the existence of disparate multi-modal ages among sedimentary inclusions at the site. These results have implications for previous reconstructions of the palaeoenvironment of the site as well as for interpretations of the possible significance of enigmatic hominin remains from Maludong for understanding the late phases of human evolutionary history in the region. We conclude that the complexities of reconstructing sedimentary history and allied challenges of dating sedimentary inclusions in caves require urgent and serious attention by archaeologists especially in light of the growing international attention being paid to later Middle and Late Pleistocene sites in tropical East Asia.

1. Introduction

Archaeologists working in karst caves are presented with a rather unique situation. On the one hand, such caves often contain Quaternary sediments with exceptionally well-preserved sequences and inclusions including artefacts, bones, plant phytoliths, charcoal and other materials owing to a range of geogenic and biogenic factors acting during sedimentation or after deposition has occurred. On the other hand, karst cave sediments can also be characterized by complex histories that aren't always immediately apparent, involving karstification and multiple sedimentary depositional processes all of which can result in their destruction or the reworking of inclusions. Major episodes in cave sedimentary histories are the direct result of the interplay between uplift, erosion and climate, with hydrological reactivation of caves possible over long time periods, keyed into palaeoclimatic shifts, and with the potential to deposit and erode sediments. In old caves, which have experienced hydrological cycles that produce alternating episodes of sedimentation and erosion over long periods of time, the resulting stratigraphic sequences may be difficult to interpret. Thus, cave sedimentary sequences can, and frequently do, violate the general principle of superposition with old remnant units such as breccias clinging to walls or cave floors or younger sedimentary units lying beneath older

---

* Corresponding author.
  E-mail address: d.curnoe@unsw.edu.au (D. Curnoe).

ones, while repeated episodes of sedimentation and erosion can also result in the reworking of older inclusions into younger sediments or the reverse situation (Simms, 1994; Curnoe et al., 2001; Piló et al., 2005; Auler et al., 2006; Hunt et al., 2015; O'Connor et al., 2017; Theden-Ringl et al., 2018). Long after sediments have formed, and in the absence of large scale post-depositional destruction or reworking, localised factors such as bioturbation or anthropogenic disturbance can also potentially impact on the integrity of sedimentary sequences. For example, insects burrowing into sediments, human occupants of caves and guano collection activities can all lead to the mixing of sediments and inclusions of different ages.

All this means that there is the ever-present potential for large dispersion in the age of materials excavated from within archaeological-bearing cave sediments or even a large offset in age between sediments and their inclusions which can lead to two potentially serious and inter-related phenomena: 1) time-averaging, and 2) uncertainties in association between dated samples and finds. A long-understood issue, time-averaging refers to an aggregation (or palimpsest) of temporally distinct inclusions within a single deposit or stratigraphic unit, resulting from the sum of the effects of natural and cultural processes acting during sedimentation over long periods of time. The spectre of time-averaging is ever present for archaeologists and becomes a more significant issue in older localities and certain geomorphological contexts where reworking of sediments is to be expected, such as caves. Time-averaging, sometimes framed as 'time perspectivism', has long been recognized as a potential (even theoretical) problem in archaeology (Behrensmeyer, 1988; Potts, 1988; Lucas, 2005; Shea, 2006; Bailey, 2007; Holdaway and Wandsnider, 2008; al-Nahar and Olszewski, 2016; Perreault, 2018).

The degree of confidence in the association between dated samples and inclusions of archaeological interest can also be understood in different ways depending on disciplinary or methodological expectations. For example, some workers will accept a shared stratigraphic, sedimentary or cultural context as providing confidence in the association between an archaeological find and dated material, while others would expect nothing less than dating of the find itself. On this note, in providing advice on the degree of certainty in association between radiocarbon (^{14}C) dating samples and archaeological finds Waterbolk (1971) developed four groups, or kinds of relationships, which ranged from "full certainty" (directly dated objects) through to "reasonable probability" (small, scattered samples from within a single cultural or sedimentary context).

It is only through the recent development and application of a range of Quaternary geochronological methods beyond ^{14}C dating such as Electron Spin Resonance, Optically Stimulated Luminescence, Uranium-series and Uranium-Lead dating that such issues are becoming better understood (Granger and Muzikar, 2001; Roberts et al., 2015; Hellstrom and Pickering, 2015; Skinner, 2015; King et al., 2016). Although, we do note that AMS ^{14}C continues to play a valuable role in assessing the temporal mixing of materials and their taphonomic history in archaeological sites especially in Europe (e.g., Wood et al., 2018). This newer suite of increasingly cost-effective methods has allowed for both a greater variety of materials from caves to be analyzed and an extension in chronostratigraphic sequences beyond the radiocarbon barrier of ~50,000 years. These approaches have been central to revealing the extent of this problem especially with respect to human remains where a number of workers have been advocating a direct dating approach for some time (e.g. Curnoe et al., 2001; Grün, 2006; Keates et al., 2007; Fu et al., 2008; Yokoyama et al., 2008; Mijares et al., 2010; Storm et al., 2013).

We would argue that without, at a minimum, the adoption of a multi-dating strategy there is the very real risk that understanding of the age of an archaeological site will incomplete, or worst still, misleading. For example, a number of studies have already highlighted instances where deposits of different age can be contemporaneous within a single cave or revealed sediments containing inclusions of

varying age which can be either older or younger than the apparent age of sediments or the bulk of the faunal or cultural materials unearthed (Simms, 1994; Curnoe et al., 2001; Piló et al., 2005; Auler et al., 2006; O'Connor et al., 2017; Theden-Ringl et al., 2018). In regions such as East Asia few important archaeological sites have been dated using multiple methods, yet over the last half decade they have begun to recast long-held models about Pleistocene human origins, specifically, the appearance time of anatomically modern humans and their temporal overlap with archaic hominins (Liu et al., 2010, 2015; Curnoe et al., 2012, 2015, 2016; Ji et al., 2013; Bae et al., 2014; Cai et al., 2017). In the absence of a multi-dating strategy including the direct-dating of human remains—which we acknowledge is not always feasible given their rarity and fragility—the possibility of error deriving from erroneous stratigraphic or depositional associations between finds and dated materials needs to be taken seriously and casts doubts over such claims.

In the present study, we illustrate some of these issues by comparing calibrated accelerator mass spectrometry (AMS) ^{14}C charcoal ages at Maludong ('red deer cave', southern China) with the results of Uranium-series (U-series) dating analyses of a sample of deer bone and tooth enamel from the site. Maludong is a small cave located on the edge of Huangjia Mountain, Hongzhai Village, about 7 km southwest of the city of Mengzi (Fig. 1). Fig. 1B shows the context of the cave, which was exposed through quarrying which stopped in 1989 prior to archaeological investigations. The modern land surface is highly karstified with extensive solution features, and Maludong Cave is situated at a shallow depth below the modern land surface comprising a small limestone plateau of low elevation. Circular solution structures in the upper part of the cave suggest that the cave was originally formed by solution, likely as a phreatic cave which formed below the water table at the time of formation. This upper section is connected to both the surface, via debris filled fractures within the surface karst, and to the lower part of the cave that was excavated. The solutional features, combined with its modern-day shallow depth, suggest that the cave itself does not relate to the modern-day landscape. What we are observing is a fragment of an old cave system which has been subsequently reactivated and infilled with one or more periods of sedimentation. Around 200 m[3] of sediment was removed during excavations undertaken by archaeologists in 1989 (Zhang et al., 1991) which exposed a 4–5 m lithostratigraphic sequence seemingly largely of anthropogenic origin (Fig. 1C) (Ji et al., 2013, 2016).

Maludong is important in palaeoanthropology because the morphology of remains from the site exhibit affinities to archaic humans or express a combination of anatomically modern human and archaic hominin traits (Fig. 2). Archaic features are most clearly seen in two specimens: partial cranium (calotte) MLDG 1704 and femur MLDG 1678 (Fig. 2). In MLDG 1704, for example, the supraorbital torus is a continuous bar of bone, lacking the bipartite form (contra Curnoe et al., 2012), is vertically thick and strongly anteriorly projecting; the vault profile is low and strongly arched; the frontal is constricted behind the postorbital area; parietals are short relative to frontal length; vault bones are thick; and the sagittal suture is simple in form, being weakly interdigitated. The proximal femur fragment MLDG 1678 exhibits small total and cortical areas at the subtrochanteric level; a relatively high platymeric index; small midshaft anteroposterior and mediolateral diameters; and a moderate pilastric index associated with the presence of a weakly developed femoral pilaster. Precisely how this combination of traits should be interpreted from a taxonomic viewpoint remains open (Curnoe et al., 2012, 2015). From a phylogenetic perspective, this unique combination can be explained in only three ways, the remains sampling: 1) a highly plesiomorphic (early or basal) anatomically modern human population; 2) an archaic hominin clade; or 3) a hybrid population resulting from interbreeding (reticulation) between anatomically modern humans and an unknown archaic species. The apparent Terminal Pleistocene age of these remains is, however, surprising when considering the plausibility of all three hypotheses.
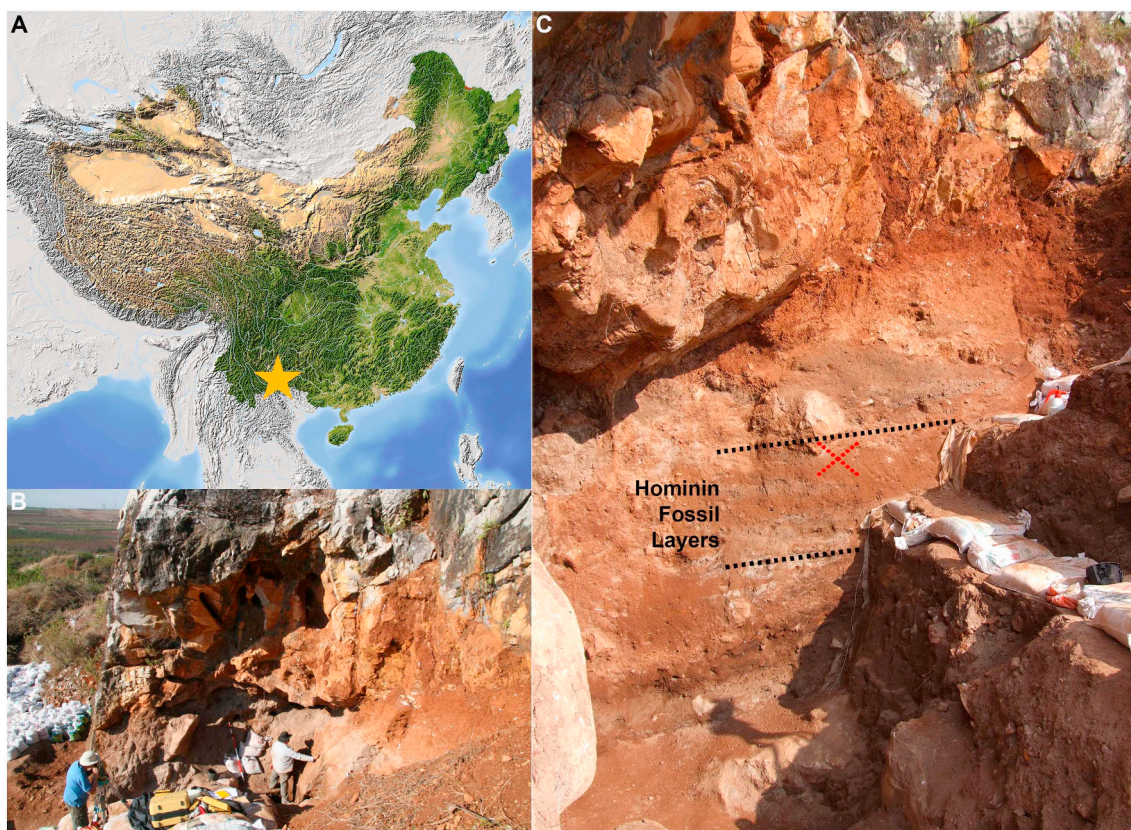
Fig. 1. Maludong palaeoanthropological site. A. Location in Southwest China (Map credit: ©Arid Ocean - stock.adobe.com). B. Site during section mapping and sampling in 2008 (with ~50% of backfill removed). C. Sedimentary sequence indicating the position of the hominin fossil-bearing layers ('X' denotes location of discovery of calotte MLDG 1704).

The basic aim of the present study is to use the complexities of the sedimentary history of Maludong as a case study for considering both the importance of applying multiple dating methods to sedimentary inclusions as well as grounds for caution in developing and testing interpretations with far reaching implications for reconstructing human evolution.

2. Materials and methods

Our first step was to calculate new calibrated AMS ^{14}C ages from charcoal collected by us at Maludong (updated from Curnoe et al., 2012; Ji et al., 2013) and compile an age-depth profile plot using OxCal v.4.2 (Ramsey, 2009) against IntCal13 (Reimer et al., 2013). Second, we obtained a random sample of deer bones and teeth derived from Units 3 and 4 of the Maludong stratigraphic sequence from the collection of the Mengzi Institute of Cultural Relics and brought to Australia for dating analysis. More specific information about provenience is lacking because the records were lost after the lead archaeologist on the original project (X. Zhang) passed away. These fragments of long bones and teeth varied in size from c10 mm to over 100 mm in length. Samples of human (n3) and the deer bone and teeth (n10) are the centre of the present study were assessed for possible AMS ^{14}C dating (by Beta Analytic and ANSTO) but in all cases the nitrogen (N%) values of < 0.1 indicated severe degradation. We further applied Uranium-series (U-series) dating analyses to these deer bone and teeth.

U-series analyses provide insights into when U has migrated into bone or tooth constituents. While this is often assumed to have occurred soon after burial, it may in fact have happen a short or long time after incorporation into a sedimentary context with later U-overprints potentially existing which can be difficult or even impossible to identify. Thus, it should be kept in mind that apparent U-series results from

bones are generally regarded to be minimum ages only, and unlike with corals and speleothems, they are based on the premise that U is taken up from the environment by bone apatite that scavenges U, but excludes Th, during diagenesis. Fresh bone contains little or no U, so U uptake can only occur post-mortem. Yet, it can be difficult to determine by how much U-series results underestimate the true age of a bone sample. In ideal cases, U uptake will have reached saturation during the early stages of fossilization (early uptake mode). In this case, a U-Th date should approximate the depositional age of the fossil (Pike et al., 2002). However, in most cases U uptake modes are likely to have been more complex (Grün, 2009). Because of the complex U-uptake history even in different parts of the same bone, apparent U-Th dates may vary across a single sample. All of them should, however, represent minimum ages of deposition, with the oldest being closest to the true burial age of the bone. In some cases, the preferential loss of U relative to Th owing to subsequent leaching of soluble U from bone may result in a ^{230}Th/^{238}U ratio that is apparently too high, leading to age overestimation (Pike et al., 2002). While such variation cannot easily be detected using conventional (solution) U-series analysis, U leaching can possibly be identified on the basis of combined U concentration and U isotope profiling across samples using the laser ablation (LA-ICPMS) method.

We have employed both the conventional (solution or isotope dilution) and LA-ICPMS methods to assess variation with geological age within individual specimens and across materials and methods. Conventional U-Th dating was conducted using a Nu Plasma multicollector inductively-coupled plasma mass spectrometer (MC-ICP-MS) in the Radiogenic Isotope Facility (RIF) at the School of Earth and Environmental Sciences, The University of Queensland following chemical treatment procedures and MC-ICP-MS analytical protocols described previously (Clark et al., 2014; Zhao et al., 2009). Fossil samples
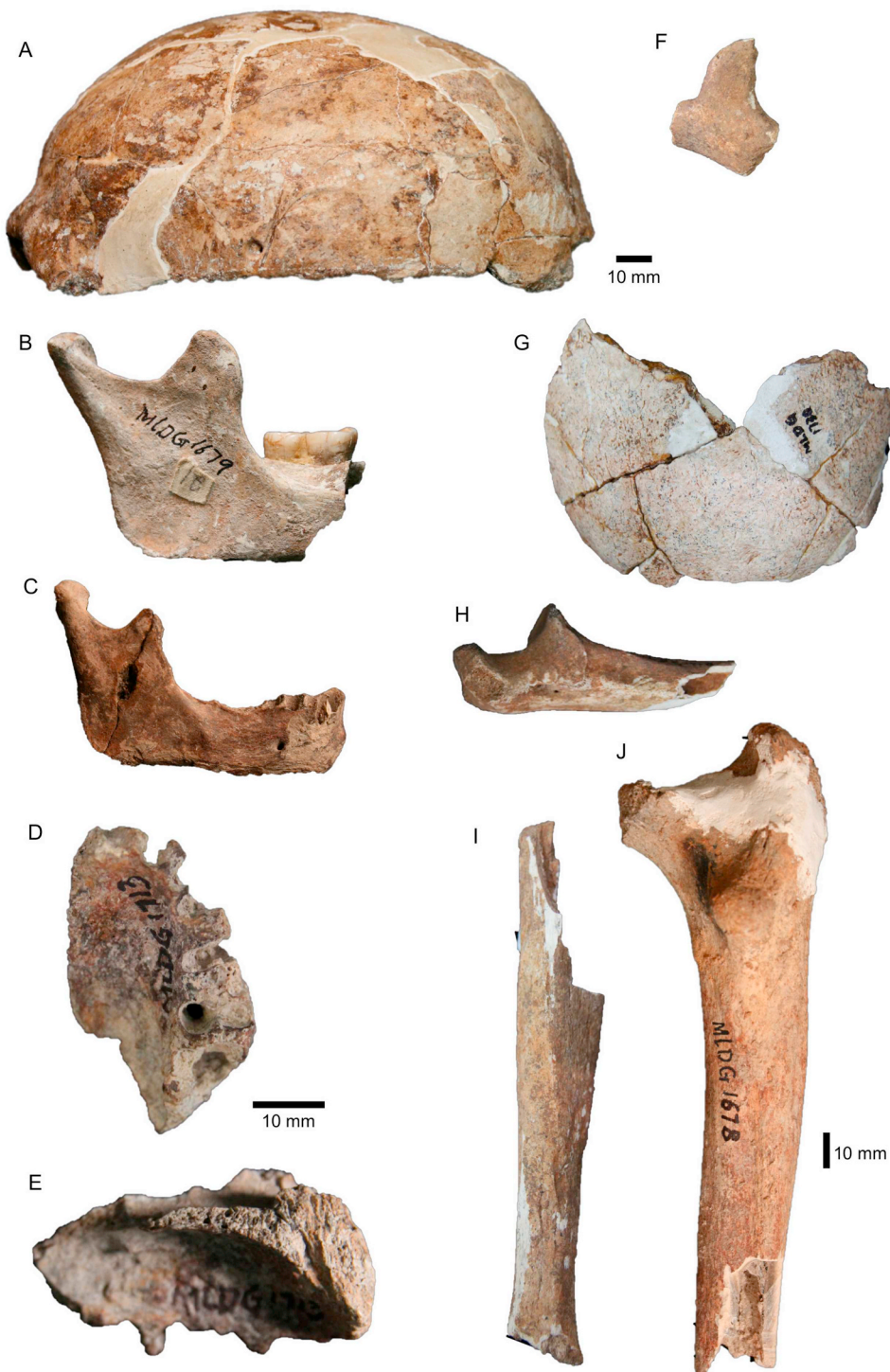
Fig. 2. Examples of hominin remains recovered from Maludong. A. Calotte MLDG 1704 (left lateral view). B. Mandible MLDG 1679 (right lateral view). C. Mandible MLDG 1706 (right lateral view). D. Juvenile maxilla MLDG 1713 (palatal view; twice natural size). E. Juvenile maxilla MLDG 1713 (sagittal; twice natural size). F. Zygomatic fragment MLDG 1708 (anterior view). G. Occipital fragment MLDG 1734 (posterior view). H. Proximal ulna fragment MLDG 1710 (lateral view). I. Tibial shaft fragment (unnumbered). J. Proximal femur fragment MLDG 1678 (posterior view).

weighing 1.5–2.5 mg were spiked with a mixed ^{229}Th-^{233}U tracer and then dissolved completely in concentrated HNO3. After digestion, each sample was treated with H_2O_2 to decompose trace amounts of organic matter and to facilitate complete sample-tracer homogenization. U and Th were separated using conventional anion-exchange column chemistry using Bio-Rad AG 1-X8 resin. After stripping off the matrix from the column using double-distilled 7 N HNO as eluent, 3 ml of a 2% HNO3 solution mixed with trace amount of HF was used to elute both U

and Th into a 3.5-ml pre-cleaned test tube, ready for MC-ICP-MS analyses, without the need for further drying down and re-mixing. After column chemistry, the U-Th mixed solution was injected into the MC-ICP-MS through a DSN-100 desolvation nebuliser system with an uptake rate of around 0.07 ml per minute. U-Th isotopic ratio measurement was performed on the MC-ICP-MS using a detector configuration to allow simultaneous measurements of both U and Th isotopes (Clark et al., 2014). The ^{230}Th/^{238}U and ^{234}U/^{238}U activity ratios of the

samples were calculated using the decay constants given in (Cheng et al., 2000). The non-radiogenic ^{230}Th was corrected using an assumed bulk-Earth atomic ^{230}Th/^{232}Th ratio of $4.4 \pm 2.2 \times 10^{-6}$. U-Th ages were calculated in *Isoplot* (Ludwig, 2012).

For LA-ICPMS, we first made a cut perpendicular to the bone/enamel surface using a rotatory tool equipped with a thin (100 µm wide) diamond saw blade. The cut sample was mounted into an aluminium cup, aligning the cross-sectioned surface with the outer rim of the sample holder to position the samples on the focal plane of the laser in the sampling cell. Sequential laser spot analyses were undertaken along two parallel tracks, starting from the interior of the cross-sectioned bone. The analyses were made at regular spacing (typically 2–3 mm) along each track, using a laser spot size of 265 µm and a 5 Hz pulse rate. The samples were initially cleaned for 5 s and ablation pits were measured for 50s. U-series ages were calculated using the *Isoplot* program (Ludwig, 2012). Closed system ages were calculated for each spot analysis and an age estimate (and the 2σ ± errors) was calculated for each parallel track and is given as a combination of standard error of the mean and average relative error. Laser ablation U-series dating was undertaken using the MC-ICP-MS system at the Australian National University's Research School of Earth Sciences. The details of LA-ICPMS analysis of skeletal remains were recently summarized in Grün et al. (2014).

3. Results

3.1. AMS radiocarbon dating

In Table 1 and Figs. 3 and 4, we present calibrated AMS ^{14}C dates on charcoal for the Maludong lithostratigraphic sequence. The entire sequence as revealed by the present-day witness section has been divided by us into six units on the basis of section mapping and on-site lithological analysis (Ji et al., 2016) and spans the period 13,390–13,140 cal BP to 18,075–17,678 cal BP (at 95.4% probability). The age-depth profile shown in Fig. 3 indicates that the formation of Units 1–4 involved a process of more or less continuous sedimentation through time, regardless of observable macroscopic lithological differences between them. For Units 1–3, all of the dates overlap at 95.4% probability, ranging from 13,720–13,461 cal BP to 13,390–13,410 cal BP. Moreover, Units 5 and 6 each would seem to represent earlier and discreet (both from each other and from Units 1–3) episodes of deposition.

Unit 1 is a brownish-red silty clay with small limestone breccia inclusions containing consolidated clay agglomerates of possible burnt

origin, a large amount of charcoal and burnt fossilized bone. AMS ^{14}C dating of charcoal places it between 13,390–13,140 cal BP and 13,595–13,399 cal BP (at 95.4% probability). Unit 2 comprises grey sandy silts partially capped by large limestone blocks with numerous combustion features and a large quantity of charcoal and red consolidated clay agglomerates of possible burnt origin. AMS ^{14}C dating of charcoal places it between 13,778–13,565 cal BP and 13,720–13,461 cal BP (at 95.4% probability). Unit 3 is a ~0.9 m thick stratigraphic aggregate (ORS + GAS subunits, Fig. 4) which contains numerous combustion features, charcoal, burnt and scorched fossils. Five AMS ^{14}C dates of charcoal collected from these combustion features dates Unit 3 from 14,048–13,753 cal BP (bottom of ORS) to 14,930–14,190 cal BP (at 95.4% probability) (bottom of GAS) (Table 1, Fig. 4). Unit 4 (ALROC + LSN, Fig. 4) is ~0.6 m thick and also contains a large quantity of charcoal as well as red consolidated clay agglomerates associated with combustion features. A single AMS ^{14}C date on charcoal from the bottom of the ALROC subunit dates it 14,656–14,052 cal BP (at 95.4% probability) (Table 1, Fig. 4). At the base of Unit 4 is a ~0.2 m sterile and undated limestone gravel unit (LSN, Fig. 4) which seals in the much older Unit 5—dated 16,500–16,022 cal BP and 16,790–16,266 cal BP (at 95.4% probability)—and Unit 6—18,075–17,678 cal BP (at 95.4% probability) (top of subunit BASE) (Table 1, Fig. 4).

All of these units except subunit LSRS (top of Unit 2) and LSN (bottom of Unit 4) contained the fossilized remains of mammals. All of the human remains were recovered from within the lower part of Unit 3 and upper section of Unit 4 (Fig. 4), and again, there is overlap at 95.4% probability for calibrated ^{14}C dates from charcoal samples suggesting they formed relatively quickly and in a more or less continuous manner.

3.2. Uranium-series dating

The results of conventional U-series dating of deer bones and teeth from Maludong are summarized in Table 2. Ages could only be calculated for seven out of 10 samples owing to evidence of uranium leaching combined with excess thorium which implies open system behaviour. Additionally, three of the 10 samples fall into the "Forbidden Zone" on the ^{230}Th/^{238}U versus ^{234}U/^{238}U evolution diagram, definitive evidence of U-series open-system behaviour indicative of uranium leaching in these samples (Fig. 5). This should be grounds for caution in their interpretation.

The U concentration of MLDG-LEAD-06 is a remarkable 5662 ppm while the apparent age for the sample of 16.4 ± 0.2 ka is an order of magnitude or more younger than all of the other samples (Table 2). Considering the fact that sample MLDG-LEAD-04 exhibited the highest U level and a significantly different ^{234}U/^{238}U ratio, it must have experienced a different uranium uptake history and U-Th disequilibrium evolution history possibly with a closed-system of decay. In this regard, its apparent age could be close to the true age of the sample and lies within the range of calibrated AMS ^{14}C ages on charcoal for the site (Tables 1). On the other hand, apparent ages for the other six dated samples, which have much lower U levels, date between 112.1 ± 0.4 ka (MLDG-LEAD-04) and 360.2 ± 3.5 ka (MLDG-LEAD-01) (Table 2). These older apparent U-Th dates could suggest they were either truly older than MLDG-LEAD-06, and thus later recycled into the same sedimentary sequence, or experienced varying degrees of uranium leaching. Without independent U-Th ages of associated speleothems in the stratigraphic context, it is a priori difficult to assess these contrasting scenarios.

LA-ICPMS U-series age calculations are summarized in Tables 3–5. U-series dates on bone are compromised if the U-concentrations are below about 0.5 ppm. In this study, each spot analysis yielded a U-concentration above 0.5 ppm. The presence of detrital ^{232}Th, which may either derive from sedimentary material within the pores of the sample or diffusion from outside sediment can also compromise the results. When the elemental U/Th ratio drops below 300 ppm the

Table 1
Calibrated ages for AMS ^{14}C dates of charcoal (calibrated using IntCal13[a]).

Lithostratigraphic unit (depth, m)	Sample no.	Conventional radiocarbon age (years BP, ± 1σ error)	From: age (cal. years BP)	To: age (cal. years BP)
1 (0.192)	OZM870	11,425 ± 50	13,390	13,140
1 (0.737)	OZM143	11,527 ± 51	13,462	13,274
1 (0.894)	OZM154	11,675 ± 52	13,595	13,399
2 (1.200)	OZM144	11,874 ± 49	13,778	13,565
2 (1.660)	OZM145	11,749 ± 49	13,720	13,461
3 (1.995)	OZM146	12,037 ± 54	14,048	13,753
3 (2.001)	OZM147	11,982 ± 78	14,050	13,600
3 (2.020)	OZM155	12,020 ± 51	14,036	13,745
3 (2.348)	OZM148	12,137 ± 51	14,161	13,816
3 (2.398)	OZM153	12,430 ± 57	14,930	14,190
4 (2.919)	OZM149	12,304 ± 59	14,656	14,052
5 (3.313)	OZM150	13,490 ± 65	16,500	16,022
5 (3.500)	OZM151	13,683 ± 62	16,790	16,266
6 (3.900)	OZM152	14,699 ± 65	18,075	17,678

[a] Further details of AMS ^{14}C age methods can be found in Curnoe et al. (2012) and above, Materials and Methods.
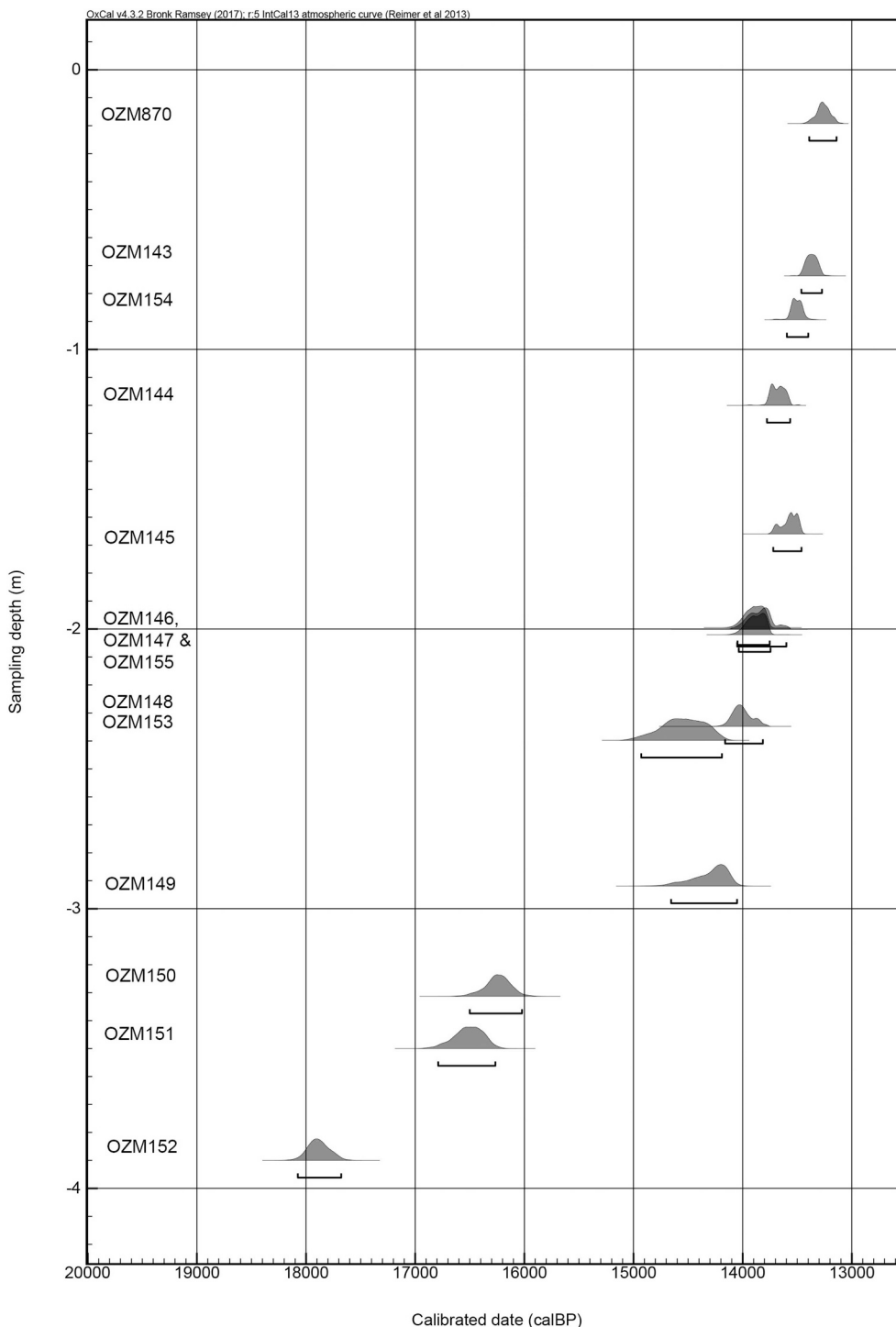
Fig. 3. Age-depth profile for calibrated AMS ^{14}C ages on charcoal from Maludong.

resulting U-series result may be influenced by detrital [230]Th and this was the case only for MLDG-LEAD-02, Line 1 at Spot-12 and Line 2 at Spot-1. However, in these locations this was associated with secondary calcium carbonate minerals located inside the middle layer of the tooth. In some cases, U may leach from the outside of the sample, but this can be recognized either by $^{230}Th/^{238}U \gg ^{234}U/^{238}U$ (all isotope ratios are given as activity ratios) or increasing U-series ages towards the outside of the tissue combined with decreasing U concentrations.

Sample MLDG-LEAD-02 (Table 3, Fig. 6) is a deer tooth and all of the sampling locations on dentine showed $^{230}Th/^{238}U$ activity ratios to be slightly higher than $^{234}U/^{238}U$ activity ratios suggesting possible

leaching of uranium. Thus, while the apparent closed system age for the dentine was around 300 ka this may be an overestimate (Fig. 6). It is noteworthy that the solution age for MLDG-LEAD-02 of 304.8 ± 1.8 ka (Table 2) is very close to the closed system age for dentine from laser ablation but again the $^{230}Th/^{238}U$ activity ratio is slightly higher than $^{234}U/^{238}U$ activity ratio indicating possible uranium loss. As enamel is generally more resistant to U leaching, dates based on this material should be more reliable. This would imply the minimum age of the specimen from enamel of 155 ± 7 ka (the mean of the five data points located solely on enamel: Line 1 Spot-4 and Spot-5, and Line 2 Spot-7, Spot-8 and Spot-9) should be taken as more trustworthy in this instance.
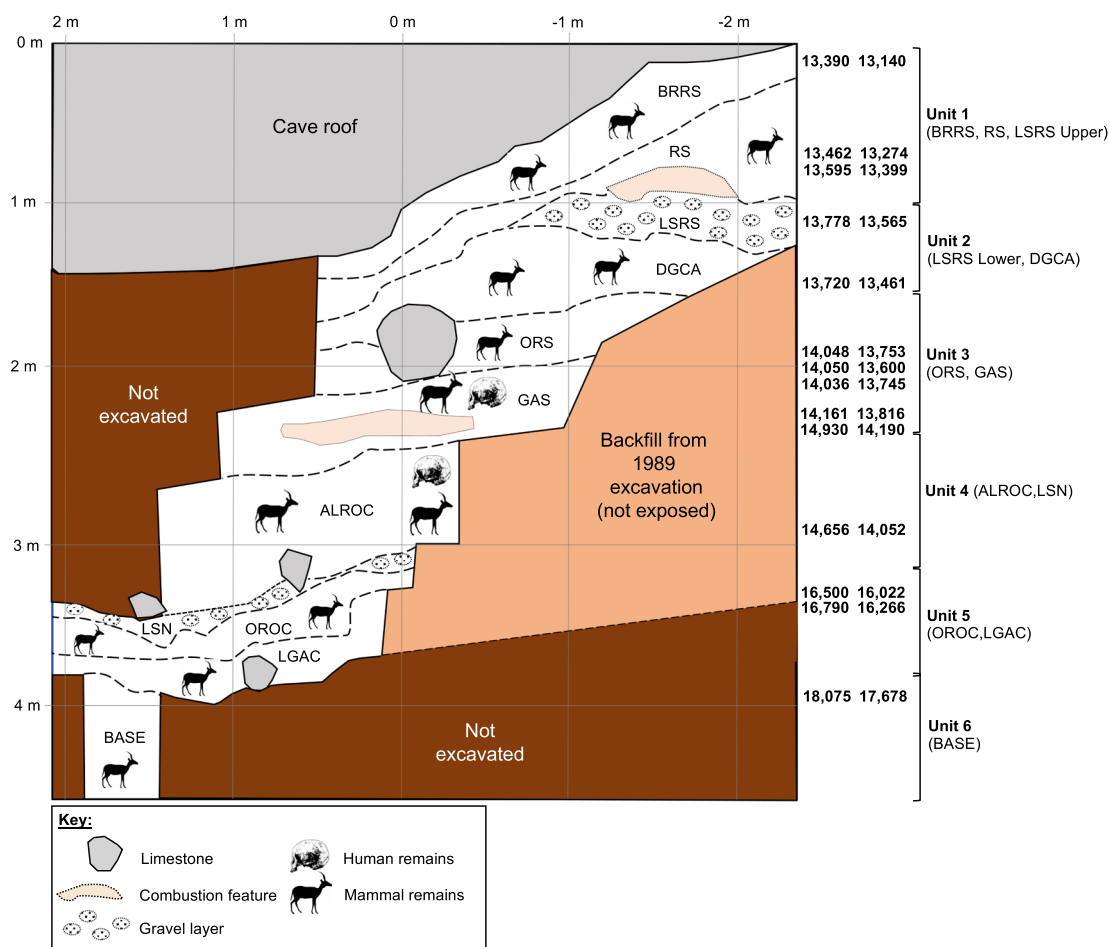
Fig. 4. Mapped Maludong witness section showing main stratigraphic divisions, provenience of human remains and calibrated AMS ^{14}C ages (cal BP) on charcoal.

The second sample analyzed was a deer bone (sample MLDG-LEAD-05) which was found to lack obvious signs of U leaching. Moreover, since there is no particular trend in the data, the minimum age of the sample is given as the mean value of all the individual spots (Table 4 and Fig. 6). The minimum age of the specimen was found to be 140 ± 2.5 ka, although, the oldest possible minimum age is about 170 ± 2.1 ka which is likely to be closer to the true age of the sample. This is close to the solution age of 163.5 ± 0.6 for the sample (Table 2). The lack of clear evidence for multiple age modes in this sample suggests that the range dates probably represents a long-term process of U-uptake lasting ~58 ka rather than temporally distinct overprints.

The final sample we analyzed with the laser ablation method was another deer bone (MLDG-LEAD-06) (Table 5, Fig. 6). It lacked obvious signs of U leaching and the data showed an increase in U concentration associated with an increase in apparent U-series ages from the inside to the outside of the bone (Fig. 6). These ages increased from 140 ± 4.1 ka to 221 ± 5.2 ka indicating that the minimum age for this sample could be as old as about 221 ka. The more conservative minimum age estimate is given as the mean value of all the individual spots, with a minimum estimate of 177 ± 5 ka. The results of solution U-series indicated some open system behaviour for this sample

Table 2
Summary of results of isotope dilution Uranium-series analyses[a].

Sample	U (ppm)	[232]Th (ppb)	([230]Th/[238]U)	± 2σ	([234]U/[238]U)	± 2σ	Corr. age (ka)	± 2σ
MLDG-LEAD-01	76.496	394.070	1.618	0.002	1.505	0.001	360.2	3.5
MLDG-LEAD-02	80.006	77.930	1.608	0.002	1.542	0.001	304.8	1.8
MLDG-LEAD-03	15.726	40.280	1.388	0.002	1.650	0.001	164.8	0.6
MLDG-LEAD-04	12.673	273.260	0.995	0.002	1.478	0.001	112.1	0.4
MLDG-LEAD-05	93.537	15.350	1.392	0.002	1.660	0.002	163.5	0.6
MLDG-LEAD-06	5662.000	109.560	0.834	0.012	5.861	0.004	16.4	0.2
MLDG-LEAD-07	77.424	256.170	1.888	0.003	1.913	0.002	229.2	1.0
MLDG-LEAD-08	30.030	31.070	3.636	0.005	2.663	0.001	Indet.	Indet.
MLDG-LEAD-09	27.632	35.530	3.773	0.007	2.814	0.002	Indet.	Indet.
MLDG-LEAD-10	35.246	16.530	3.763	0.005	2.807	0.002	Indet.	Indet.

  [a] Ratios listed in the table refer to activity ratios normalized to the corresponding ratios measured for the secular-equilibrium HU-1 standard. [230]Th ages are calculated using Isoplot/Ex 3.75 [36], using decay constants of (Cheng et al., 2000). Non-radiogenic [230]Th correction was applied assuming non-radiogenic [230]Th/[232]Th atomic ratio = 4.4 ± 2.2 × 10^{-6} (bulk-earth value), and [238]U, [234]U, [232]Th and [230]Th are in secular equilibrium. uncorr. and corr. denote uncorrected and corrected.
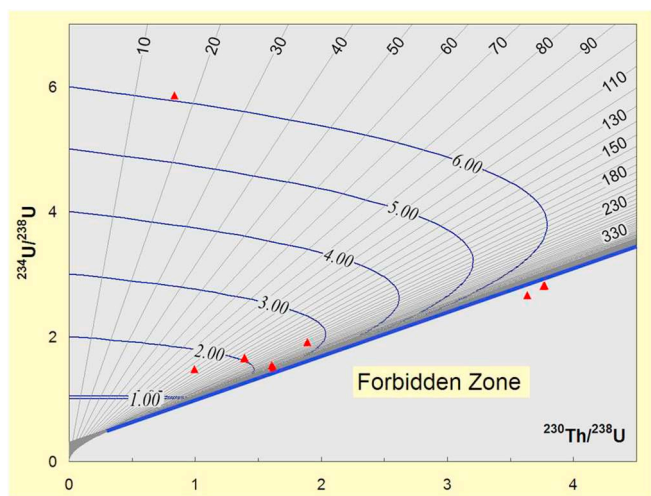
Fig. 5. ^{230}Th/^{238}U versus ^{234}U/^{238}U evolution diagram with labelled evolution curves and isochrons (after Ludwig, 2012). The heavy blue straight line represents closed-system evolution form an 'infinite' ^{234}U/^{238}U activity ratio at an 'infinite' age. The area to the right of this line has isotopic compositions that are impossible to achieve through closed-system decay and is therefore considered to be the "Forbidden Zone." Note that three fossil samples fall into the "Forbidden Zone" implying definitive open-system behaviour. (For interpretation of the references to colour in this figure legend, the reader is referred to the web version of this article.)

implying an erroneous age. While along the transect the age estimates are largely within error of each other, the ages from this single sample do cover a considerable range from 132 to 231 ka (at 95.4% confidence). Again, this would imply a long-term process of U-uptake lasting ~99 ka rather than temporally distinct overprinting.

Laser-ablation profiling was undertaken to determine the uranium

uptake mode and whether U leaching had occurred. The three samples dated by LA-ICPMS do not fall into the forbidden zone, while three tooth samples dated by solution do; conclusive evidence for U leaching or Th gain (i.e. excess daughter ^{230}Th unsupported by parental ^{234}U or ^{238}U). However, samples that do not fall into forbidden zone and still provide ages may still have been affected by U leaching. For such samples, the future application of LA-ICPMS profiling would be insightful. It is not possible to model U-diffusion through teeth because of the 3-dimensional nature of U uptake in such material. Besides, the age profiles are relatively flat in both the dentine and the other bone samples analyzed here. Modelling the uranium uptake in such samples could potentially only provide slightly older minimum ages and would have minimal impact on the results.

4. Discussion and conclusions

The results of U-series dating on deer bone and tooth samples from Maludong highlight an unexpected spread in apparent ages for sedimentary fossils recovered from the site. AMS ^{14}C ages for charcoal sampled from in situ combustion features within Units 3 and 4 of the preserved witness section indicate the sediments were deposited during the post-LGM (post-Last Glacial Maximum) phase of the Late Pleistocene (i.e. 13,390–13,140 cal BP to 18,075–17,678 cal BP, at 95.4% probability). Strikingly, U-series analysis of a small and randomly selected sample of deer bones and teeth excavated from within these units has provided apparent ages within the range of 16.4 ± 0.2 ka to 360.3 ± 3.5 ka (conventional) and 169.3 ± 2.1 ka to 481 + 28/−23.7 ka (LA-ICPMS). However, in taking into account evidence for likely open-system behaviour in some of the samples, this range is reduced substantially to between 112 ± 0.4 ka and 177 ± 5 ka. This represents a period of around 65 ka in contrast to the much smaller duration sampled by AMS ^{14}C ages on charcoal of ~4.5–4.7 ka. Moreover, the offset in age between the charcoal and fossil ages is rather remarkably in the range of around 95–164 ka.

Table 3
Summary of LA-ICPMS results for sample MLDG-LEAD-02 (deer tooth).

Spot	U (ppm)	^{232}Th (ppb)[a]	(^{230}Th/^{238}U)	± 2σ	(^{234}U/^{238}U)	± 2σ	Age (ka)	+ 2σ	− 2σ
1	65.0000	29.2000	1.6041	0.0161	1.5420	0.0047	301.20	13.60	12.50
2	84.9700	0.6800	1.5943	0.0157	1.5493	0.0017	287.70	11.30	10.40
3	57.2100	0.3400	1.4831	0.0141	1.5349	0.0026	235.10	6.80	6.50
4	4.2500	0.0100	1.0217	0.0153	1.2954	0.0077	153.70	5.20	5.00
5	0.5800	0.0700	0.9772	0.0566	1.5068	0.0390	105.50	11.20	10.30
6	30.9900	1.5600	1.5361	0.0191	1.5364	0.0029	261.20	11.40	10.50
7	50.3200	1.0800	1.5686	0.0161	1.5489	0.0029	271.60	10.30	9.60
8	59.2400	2.7400	1.6032	0.0157	1.5423	0.0034	300.30	12.90	11.80
9	50.5800	2.2300	1.6070	0.0109	1.5519	0.0057	294.40	9.50	9.00
10	55.9000	3.4600	1.6289	0.0169	1.5559	0.0038	307.10	14.50	13.20
11	37.1600	50.5300	1.6296	0.0086	1.5587	0.0036	305.00	7.70	7.30
12	1.0800	66.0300	0.6663	0.0241	1.5093	0.0171	61.20	3.10	3.00
13	0.5000	1.9400	0.6874	0.0313	1.3696	0.0233	73.20	5.00	4.80
14	20.8500	60.9800	1.6329	0.0151	1.5496	0.0032	316.80	13.90	12.70
15	57.8000	5.6300	1.6533	0.0125	1.5520	0.0023	332.40	12.80	11.80
16	59.9500	3.2300	1.6270	0.0152	1.5471	0.0026	314.40	13.60	12.40
17	57.4400	2.2300	1.5651	0.0076	1.5309	0.0033	283.00	5.90	5.70
18	27.9300	0.7300	1.5111	0.0102	1.5190	0.0033	258.50	6.30	6.00
19	2.9900	−0.0600	1.2881	0.0167	1.5396	0.0080	165.60	5.00	4.80
20	2.8400	0.0500	1.3433	0.0218	1.5443	0.0088	179.90	7.20	6.80
21	5.0900	0.0000	1.2737	0.0143	1.5021	0.0079	171.50	4.80	4.60
22	58.7700	1.9600	1.5501	0.0080	1.5102	0.0026	290.10	6.30	6.10
23	56.6300	27.9100	1.5755	0.0060	1.5189	0.0022	301.10	5.20	5.00
24	66.7000	50.9600	1.7585	0.0087	1.5599	0.0019	481.00	28.00	23.70
25	70.2400	58.2000	1.6155	0.0129	1.5371	0.0019	315.30	11.60	10.70
26	73.0200	74.6100	1.5485	0.0104	1.5314	0.0022	272.00	6.80	6.40
27	75.2600	57.5900	1.5710	0.0181	1.5195	0.0018	297.10	14.50	13.10
28	78.2900	5.6500	1.5269	0.0184	1.5191	0.0026	267.70	11.80	10.80
29	66.5000	44.6200	1.6506	0.0137	1.4961	0.0026	430.20	33.40	27.20
30	60.0600	178.6500	1.5553	0.0107	1.4771	0.0027	329.50	11.80	11.00

[a] Negative values due to background over-correction.

Table 4
Summary of LA-ICPMS results for sample MLDG-LEAD-05 (deer bone).

Spot	U (ppm)	^{232}Th (ppb)[a]	(^{230}Th/^{238}U)	± 2σ	(^{234}U/^{238}U)	± 2σ	Age (ka)	+ 2σ	− 2σ
1	48.3900	3.4600	1.3290	0.0224	1.6735	0.0028	146.7	4.8	4.6
2	57.7900	3.9800	1.4172	0.0167	1.6773	0.0019	165.6	4.1	4.0
3	68.0700	0.8700	1.3696	0.0164	1.6732	0.0019	155.5	3.7	3.6
4	65.7000	0.5200	1.3000	0.0144	1.6717	0.0023	141.1	2.9	2.9
5	55.8700	1.6200	1.2940	0.0176	1.6741	0.0024	139.5	3.5	3.4
6	46.7400	1.5800	1.3660	0.0130	1.6710	0.0023	155.1	3.0	2.9
7	52.2300	1.1500	1.3264	0.0094	1.6635	0.0019	148.0	2.0	2.0
8	55.5600	− 0.0400	1.2661	0.0168	1.6656	0.0022	135.5	3.3	3.2
9	54.0500	0.3300	1.3002	0.0107	1.6650	0.0022	142.3	2.2	2.2
10	55.7300	0.0300	1.2748	0.0093	1.6609	0.0029	138.0	1.9	1.9
11	46.9700	− 0.0800	1.2453	0.0079	1.6674	0.0021	131.3	1.5	1.5
12	56.3100	0.2200	1.2478	0.0135	1.6724	0.0028	131.0	2.5	2.5
13	52.2500	0.1200	1.3065	0.0094	1.6730	0.0025	142.2	1.9	1.9
14	62.8400	0.5800	1.4224	0.0108	1.6766	0.0018	167.0	2.7	2.6
15	65.9300	0.3100	1.4401	0.0084	1.6849	0.0021	169.3	2.1	2.1
16	57.2800	0.6500	1.3408	0.0196	1.6809	0.0027	147.8	4.2	4.0
17	64.3500	0.6900	1.3003	0.0190	1.6710	0.0026	141.3	3.9	3.8
18	49.6400	9.7300	1.2921	0.0127	1.6714	0.0016	139.6	2.5	2.5
19	59.4200	0.8700	1.2622	0.0129	1.6761	0.0024	133.1	2.5	2.4
20	56.2900	0.4900	1.2652	0.0091	1.6759	0.0023	133.7	1.8	1.7
21	57.6900	0.6600	1.2996	0.0126	1.6718	0.0024	141.0	2.6	2.5
22	50.0300	0.5900	1.2875	0.0091	1.6720	0.0031	138.6	1.9	1.8
23	57.3800	0.4000	1.2085	0.0103	1.6646	0.0026	125.1	1.9	1.8
24	53.4600	0.1200	1.2295	0.0109	1.6714	0.0024	127.9	2.0	2.0
25	55.0500	0.0900	1.1893	0.0083	1.6610	0.0021	122.2	1.5	1.5
26	57.1900	− 0.0700	1.1769	0.0080	1.6711	0.0025	118.8	1.4	1.4
27	61.9600	0.4800	1.1923	0.0075	1.6675	0.0022	121.9	1.3	1.3
28	61.2600	0.0600	1.1939	0.0085	1.6699	0.0031	121.8	1.5	1.5
29	64.8600	0.8200	1.2773	0.0174	1.6794	0.0019	135.4	3.3	3.3
30	70.8100	0.6600	1.4382	0.0112	1.6858	0.0020	168.7	2.8	2.7

[a] Negative values due to background over-correction.

We suggest that the presence of likely late Middle to early Late Pleistocene fossil inclusions within the apparently later Late Pleistocene sediments at Maludong is the result of reworking. They would seem to have derived from an earlier phase of deposition associated with a stratigraphic unit that was subsequently eroded. This erosional event is likely to have happened as part of the second phase of sedimentation which occurred during the formation of the Late Pleistocene lithostratigraphic section present today at the locality. Such a scenario would be supported by dating analyses for sample MLDG-LEAD-06 with its very high U concentration (5662 ppm) and young (conventional) U-series age of 16.4 ± 0.2 ka implying likely closed system behaviour. Alternatively, these samples could have originated from within an unrecognized lithological unit removed completely during the original excavations and with no trace of it in the witness section. This seems

less likely given that the previous descriptions of the lithostratigraphic sequence broadly match our own investigations of the sediments at Maludong (Zhang et al., 1991; Curnoe et al., 2012; Ji et al., 2013, 2016).

Previous U-series dating of speleothem samples from Maludong have provided age estimates of ~45 ka for a layer formed on the ceiling of the cave and an open-ended date of > 630 ka for crystalline calcite from the lower part of the Maludong sedimentary sequence (Ji et al., 2013). We have previously interpreted these to indicate the age when the cave may have opened, in the case of the former, and the age of the original vein fill of the fault on which the cave was formed, for the later (Ji et al., 2013). This model for Maludong needs to be revised somewhat in light of our new U-series dates. Our new dates on deer bones and teeth suggest instead that the cave was probably opened to the surface
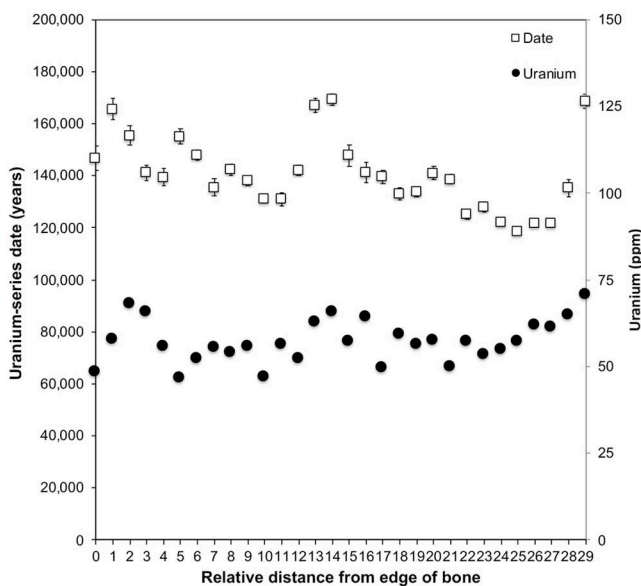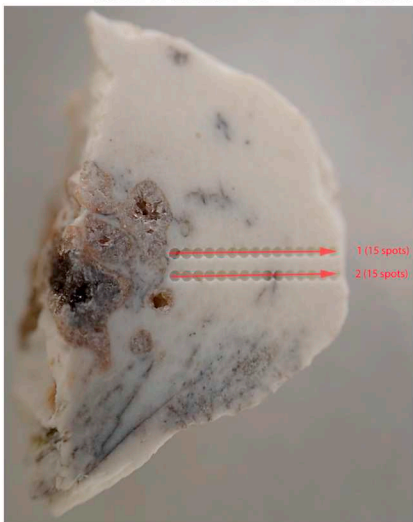
Table 5
Summary of LA-ICPMS results for sample MLDG-LEAD-06 (deer bone).

| Spot	U (ppm)	^{232}Th (ppb)	(^{230}Th/^{238}U)	± 2σ	(^{234}U/^{238}U)	± 2σ	Age (ka)	+ 2σ	− 2σ
1	29.060	2.550	1.588	0.026	2.015	0.004	140.3	4.1	4.0
2	29.940	0.660	1.721	0.024	2.017	0.004	162.6	4.6	4.5
3	38.900	0.240	1.723	0.029	2.004	0.003	165.3	5.6	5.4
4	38.220	0.750	1.625	0.023	1.984	0.005	150.9	4.1	4.0
5	34.830	0.280	1.671	0.021	1.952	0.005	164.6	4.3	4.2
6	26.520	0.630	1.796	0.023	1.907	0.009	203.6	7.0	6.7
7	47.770	0.820	1.907	0.017	1.954	0.004	220.9	5.2	5.0
8	50.330	1.420	1.867	0.011	1.951	0.002	210.3	3.1	3.0
9	30.990	0.910	1.742	0.026	2.015	0.004	166.9	5.0	4.9
10	31.070	21.540	1.657	0.017	2.014	0.004	151.7	3.0	3.0
11	39.710	1.080	1.744	0.021	2.013	0.003	167.6	4.1	4.0
12	38.550	0.300	1.724	0.025	2.010	0.004	164.4	4.9	4.8
13	39.360	0.720	1.764	0.021	1.988	0.003	176.7	4.5	4.4
14	39.650	1.080	1.839	0.017	1.953	0.006	202.2	4.8	4.6
15	35.010	0.490	1.690	0.036	1.935	0.005	171.7	7.8	7.4
16	35.190	1.070	1.663	0.022	1.925	0.005	168.1	4.6	4.5
17	41.770	1.010	1.799	0.021	1.945	0.003	194.3	5.2	5.0
18	50.130	3.350	1.860	0.016	1.945	0.003	210.0	4.4	4.3

MLDG-LEAD-02 – Deer tooth enamel
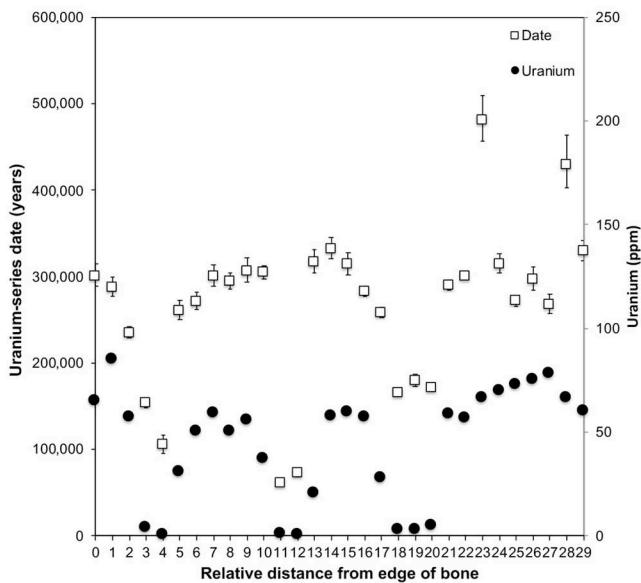
MLDG-LEAD-05 – Deer bone

MLDG-LEAD-06 – Deer bone
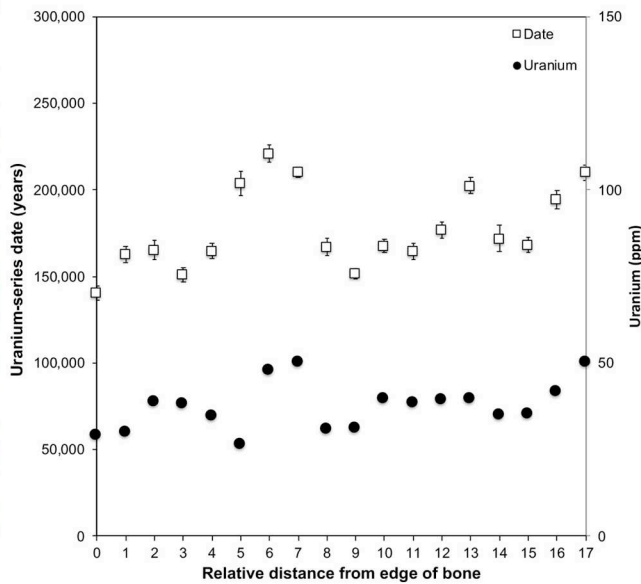
(caption on next page)

Fig. 6. Laser tracks and Uranium content and U-series age profiles for three deer samples from Maludong: MLDG-LEAD-02 (top), MLDG-LEAD-05 (middle) and MLDG-LEAD-06 (bottom). Errors on individual dates are 2σ.

Table 6
Summary of results of stable isotope analysis for deer samples from Maludong with reliable U-series dating results and indicating Marine Iotope Stage.

Sample	Preferred U-series age (ka)	$\delta^{13}C_{VPDB}$ sample average[a]	$\delta^{18}O_{VSMOW}$ sample average[a,b]	Marine Isotope Stage
MLDG-LEAD-02	155 ± 7	−19.87	22.85	6
MLDG-LEAD-04	112 ± 0.4	−19.92	21.88	5
MLDG-LEAD-05[c]	170 ± 2.1	−21.34	25.15	6
MLDG-LEAD-06	177 ± 5	−18.30	21.97	6

[a] Average of two replicates.
[b] Slightly different to previous results owing to impact of rounding.
[c] Sample not included in Ji et al. (2016).

during the Middle Pleistocene and may have been fully opened by about ~45 ka with later infilling by sediments after approximately 18 ka. This younger (later Late Pleistocene) sediment with clear signs of human occupation (in situ combustion features) contains much older inclusions (fossils) dating from the Middle Pleistocene.

Our new dating research at Maludong also indicates that the faunal assemblage from the site probably contains time-averaged elements. When we previously examined the 22 mammal fauna from Maludong only four had been identified definitively to the species level and are potentially informative about the age of the site: *Ursus thibetanus, Dicerorhinus sumatrensis*, *Sus scrofa* and *Axis porcinus* (Ji et al., 2016). However, all of them, as well as the remaining identified genera, have all been recovered from Early to Late Pleistocene deposits in East Asia (Long et al., 1996; Louys et al., 2007; Tong and Guérin, 2009) and therefore offer no obvious insights into the possible age of the Maludong deposits.

We have previously also undertaken stable isotope analysis of a number of the present deer samples and these were interpreted on the basis of the original ^{14}C AMS dating chronostratigraphic sequence which placed them all within MIS 2 (see Ji et al., 2016). In Table 6, we summarize our δ^{13}C and δ^{18}O results for them and place them within our new apparent chronological framework and assign them to a Marine Isotope Stage (MIS). Our new direct-dates clearly alter our previous interpretations with samples MLDG-LEAD-02 and MLDG-LEAD-05 (perhaps also MLDG-LEAD-06) now most likely situated within the MIS 6 interglacial and MLDG-LEAD-04 within the MIS 5e interglacial sub-stage. This is consistent with palaeoclimatic interpretations from δ^{13}C and δ^{18}O values from all of these specimens indicating that they sample warm and wet conditions with high rainfall. Thus, the implication of our results is that climatic conditions during the late Middle-early Late Pleistocene around Maludong were similar to or perhaps even wetter than experienced today.

Our revised ages for these Maludong fossils also have important implications for the enigmatic hominin remains recovered from the site and interpretations about their possible place in human evolution. All of them were recovered from Unit 3 and the upper part of Unit 4 of the Maludong lithostratigraphic sequence (dated deer samples were originally excavated from Units 3 and 4). We have described a large number of archaic or unique traits in the cranial remains from Maludong (e.g. MLDG 1679, 1704, 1705, 1706 and 1747) (Curnoe et al., 2012; Ji et al., 2013). Moreover, the partial femur from the site (MLDG 1678) also exhibits a large number of archaic features and is phenetically most similar to Lower Pleistocene hominins (Curnoe et al., 2015). The unusual morphology of these remains has been confirmed by other researchers who have even noted similarities of MLDG 1678 to australopith femora (Schwartz, 2016). It seems possible in light of our new U-series dates that at least some of these human remains may in fact derive from the later Middle Pleistocene, as would be implied by

their morphology. Clearly, given that AMS ^{14}C failed, a future priority must be to attempt to directly date some of the human remains from Maludong using the U-series method, including employing the LA-ICPMS approach, which to the best of our knowledge has not until the present study been applied to bones from archaeological sites in China.

Finally, our work brings into sharp focus the complexities of reconstructing the sedimentary history and the allied problem of dating in caves located in tropical/semi-tropical areas such as southern China. In such areas, karstification and sedimentation would have been rapid within a context of active hydrological regimes over long periods during the Pleistocene. Maludong, a near-surface, sediment-filled cave, with solution features indicative of formation in the phreatic zone, is clearly of great antiquity. Landscape erosion and associated karstification have led to the land-surface lowering to a modern-day elevation close to that of the cave. The associated reactivation of the cave over the late Quaternary has led to the deposition of the Maludong fossil units.

Southern China is currently at the centre of controversial claims for the early appearance of anatomically modern humans in East Asia during the period ~139–70 ka (Wu et al., 2006; Liu et al., 2010, 2015; Bae et al., 2014; Curnoe et al., 2016; Michel et al., 2016; Cai et al., 2017). Archaeologists working in the region continue to prefer to apply U-series dating of speleothem layers for inferring the age of Pleistocene human remains (Michel et al., 2016). The complexities of sedimentary history at sites like Maludong highlights the possible errors that can arise from the continued use of such indirect dating approaches to estimating the age of sedimentary inclusions. There is clearly an urgent need to implement wide-ranging dating strategies involving multiple approaches and materials, including minimally invasive methods like LA-ICPMS U-series and AMS ^{14}C dating directly to human remains themselves. In the case of Maludong, this will be critical to determining the true age of these highly unusual remains and to finally resolving their phyletic position.

Acknowledgements

References

al-Nahar, M., Olszewski, D.I., 2016. Early Epipaleolithic lithics, time-averaging, and site interpretations: Wadi al-Hasa region, Western Highlands of Jordan. Quat. Int. 396, 40–51.

Auler, A.S., Piló, L.B., Smart, P.L., Wang, X., Hoffmann, D., Richards, D.A., Edwards, R.L., Neves, W.A., Cheng, H., 2006. U-series dating and taphonomy of Quaternary vertebrates from Brazilian caves. Palaeogeogr. Palaeoclimatol. Palaeoecol. 240, 508–522.

Bae, C.J., Wang, W., Zhao, J., Huang, S., Tian, F., Shen, G., 2014. Modern human teeth from Late Pleistocene Luna cave (Guangxi, China). Quat. Int. 354, 169–183.

Bailey, G., 2007. Time perspectives, palimpsests and the archaeology of time. J. Anthropol. Archaeol. 26, 198–223.

Behrensmeyer, A.K., 1988. Taphonomy and hunting. In: Nitecki, M.H., Nitecki, D.V. (Eds.), The Evolution of Human Hunting. Springer, Boston MA, pp. 423–450.

Cai, Y., Qiang, X., Wang, X., Jin, C., Wang, Y., Zhang, Y., Trinkaus, E., An, Z., 2017. The age of human remains and associated fauna from Zhiren Cave in Guangxi, southern China. Quat. Int. 434 (Part A), 84–91.

Cheng, H., Edwards, R.L., Hoff, J., Gallup, C.D., Richards, D.A., Asmerom, Y., 2000. The half-lives of uranium-234 and thorium-230. Chem. Geol. 169, 17–33.

Clark, T.R., Zhao, J.-x., Roff, G., Feng, Y.-X., Done, T.J., Nothdurft, L.D., Pandolfi, J.M., 2014. Discerning the timing and cause of historical mortality events in modern Porites from the Great Barrier Reef. Geochim. Cosmochim. Acta 138, 57–80.

Curnoe, D., Grün, R., Taylor, L., Thackeray, F., 2001. Direct ESR dating of a Pliocene Hominin from Swartkrans. J. Hum. Evol. 40, 379–391.

Curnoe, D., Xueping, J., Herries, A.I.R., Kanning, B., Taçon, P.S.C., Zhende, B., Fink, D., Yunsheng, Z., Hellstrom, J., Yun, L., Cassis, G., Bing, S., Wroe, S., Shi, H., Parr, W.C.H., Shengmin, H., Rogers, N., 2012. Human remains from the Pleistocene-Holocene transition of Southwest China suggest a complex evolutionary history for east Asians. PLoS One 7, e31918.

Curnoe, D., Ji, X., Liu, W., Bao, Z., Taçon, P.S.C., Ren, L., 2015. A hominin femur with archaic affinities from the Late Pleistocene of Southwest China. PLoS One 10, e0143332.

Curnoe, D., Xueping, J., Hu, S., Taçon, P., Li, Y., 2016. Dental remains from Longtanshan Cave 1 (Yunnan, China), and the initial presence of anatomically modern humans in East Asia. Quat. Int. 400, 180–186.

Fu, R., Shen, G., He, J., Ren, H., Feng, Y.X., Zhao, J.X., 2008. Modern *Homo sapiens* skeleton from Qianyang Cave in Liaoning, northeastern China and its U-series dating. J. Hum. Evol. 55, 349–352.

Granger, D.E., Muzikar, P.F., 2001. Dating sediment burial with *in situ*-produced cosmogenic nuclides: theory, techniques, and limitations. Earth Planet. Sci. Lett. 188, 269–281.

Grün, R., 2006. Direct dating of human fossils. Am. J. Phys. Anthropol. 131 (S43), 2–48.

Grün, R., 2009. The relevance of parametric U-uptake models in ESR age calculations. Radiat. Meas. 44, 472–476.

Grün, R., Eggins, S., Kinsley, L., Moseley, H., Sambridge, M., 2014. Laser ablation U-series analysis of fossil bones and teeth. Palaeogeogr. Palaeoclimatol. Palaeoecol. 416, 150–167.

Hellstrom, J., Pickering, R., 2015. Recent advances and future prospects of the U-Th and U-Pb chronometers applicable to archaeology. J. Archaeol. Sci. 56, 32–40.

Holdaway, S., Wandsnider, L. (Eds.), 2008. Time in Archaeology. The University of Utah Press, Salt Lake City.

Hunt, C.O., Gilbertson, D.D., Hill, E.D., Simpson, D., 2015. Sedimentation, re-sedimentation and chronologies in archaeologically-important caves: problems and prospects. J. Archaeol. Sci. 56, 109–116.

Ji, X., Curnoe, D., Bao, Z.D., Herries, A.I.R., Fink, D., Zhu, Y.S., Hellstrom, J., Luo, Y., Tacon, P.S.C., 2013. Further geological and palaeoanthropological investigations at the Maludong hominin site, Yunnan Province, Southwest China. Chin. Sci. Bull. 58, 4472–4485.

Ji, X., Curnoe, D., Taçon, P.S.C., Zhende, B., Ren, L., Mendoza, R., Tong, H., Ge, J., Deng, C., Adler, L., Baker, A., Du, B., 2016. Cave use and palaeoecology at Maludong (Red Deer Cave), Yunnan, China. J. Archaeol. Sci. Rep. 8, 277–283.

Keates, S.G., Hodgins, G.W., Kuzmin, Y.V., Orlova, L.A., 2007. First direct dating of a presumed Pleistocene hominid from China: AMS radiocarbon age of a femur from the Ordos Plateau. J. Hum. Evol. 53, 1–5.

King, G.E., Guralnik, B., Vallac, P.G., Herman, F., 2016. Trapped-charge thermochronometry and thermometry: a status review. Chem. Geol. 446, 3–17.

Liu, W., Jin, C.-Z., Zhang, Y.-Q., Cai, Y.-J., Xing, S., Wu, X.-J., Cheng, H., Edwards, R.L., Pan, W.-S., Qin, D.-G., An, Z.-S., Trinkaus, E., Wu, X.-Z., 2010. Human remains from Zhirendong, South China, and modern human emergence in East Asia. Proc. Natl. Acad. Sci. 107, 19201–19206.

Liu, W., Martinón-Torres, M., Cai, Y.J., Xing, S., Tong, H.W., Pei, S.W., Sier, M.J., Wu, X.H., Edwards, R.L., Cheng, H., Li, Y.Y., Yang, X.X., De Castro, J.M.B., Wu, X.J., 2015. The earliest unequivocally modern humans in southern China. Nature 526, 696–699.

Long, V.T., de Vos, J., Ciochon, R.L., 1996. The fossil mammal fauna of the Lang Trang caves, Vietnam, compared with Southeast Asian fossil and recent mammal faunas: the geographical implications. Bull. Indo-Pac. Prehistory Assoc. 14, 101–109.

Louys, J., Curnoe, D., Tong, H., 2007. Characteristics of Pleistocene megafauna extinctions in Southeast Asia. Palaeogeogr. Palaeoclimatol. Palaeoecol. 243, 152–173.

Lucas, G., 2005. The Archaeology of Time. Routledge, London.

Ludwig, K., 2012. User's Manual for Isoplot/Ex version 3.75: A Geochronological Toolkit for Microsoft Excel. In: Berkeley Geochronology Center Special Publication No. 5.

Michel, V., Valladas, H., Shen, G., Wang, W., Zhao, J., Shen, C., Valensi, P., Bae, C., 2016. The earliest modern *Homo sapiens* in China? J. Hum. Evol. 101, 101–104.

Mijares, A.S., Détroit, F., Piper, P., Grün, R., Bellwood, P., Aubert, M., Champion, G., Cuevas, N., Leon, A. De, Dizon, E., 2010. New evidence for a 67,000-year-old human presence at Callao Cave. J. Hum. Evol. 59, 123–132.

O'Connor, S., Barham, A., Aplin, K., Maloney, T., 2017. Cave stratigraphies and cave breccias: implications for sediment accumulation and removal models and interpreting the record of human occupation. J. Archaeol. Sci. 77, 143–159.

Perreault, C., 2018. Time-averaging slows down rates of change in the archaeological record. J. Archaeol. Method Theory 25, 953–964.

Pike, A.W.G., Hedges, R.E.M., Van calsteren, P., 2002. U-series dating of bone using the diffusion-adsorption model. Geochim. Cosmochim. Acta 66, 4273–4286.

Piló, L.B., Auler, A.S., Neves, W.A., Wang, X., Cheng, H., Edwards, L.R., 2005. Geochronology, sediment provenance, and fossil emplacement at Sumidouro Cave, a classic late Pleistocene/early Holocene paleoanthropological site in eastern Brazil. Geoarchaeology 20, 751–764.

Potts, R., 1988. On an early hominid scavenging niche. Curr. Anthropol. 29, 153–155.

Ramsey, C.B., 2009. Bayesian analysis of radiocarbon dates. Radiocarbon 51, 337–360.

Reimer, P.J., Bard, E., Bayliss, A., Beck, J.W., Blackwell, P.G., Ramsey, C.B., Buck, C.E., Cheng, H., Edwards, R.L., Friedrich, M., Grootes, P.M., Guilderson, T.P., Haflidason, H., Hajdas, I., Hatté, C., Heaton, T.J., Hoffmann, D.L., Hogg, A.G., Hughen, K.A., Kaiser, K.F., Kromer, B., Manning, S.W., Niu, M., Reimer, R.W., Richards, D.A., Scott, E.M., Southon, J.R., Staff, R.A., Turney, C.S.M., van der Plicht, J., 2013. IntCal13 and Marine13 radiocarbon age calibration curves 0–50,000 years cal BP. Radiocarbon 55, 1869–1887.

Roberts, R.G., Jacobs, Z., Jankowsk, N.R., Cunningh, A.C., Rosenfeld, A.B., 2015. Optical dating in archaeology: thirty years in retrospect and grand challenges for the future. J. Archaeol. Sci. 56, 41–60.

Schwartz, J.H., 2016. What constitutes *Homo sapiens*? Morphology versus received wisdom. J. Anthropol. Sci. 94, 1–16.

Shea, J.J., 2006. Child's play: reflections on the invisibility of children in the paleolithic record. Evol. Anthropol. 15, 212–216.

Simms, M.J., 1994. Emplacement and preservation of vertebrates in caves and fissures. Zool. J. Linnean Soc. 112, 261–283.

Skinner, A., 2015. Electron Spin Resonance (ESR) dating, general principles. In: Rink, J., Thompson, J.W. (Eds.), Encyclopedia of Scientific Dating Methods. Encyclopedia of Earth Science Series. Springer, Dordrecht.

Storm, P., Wood, R., Stringer, C., Bartsiokas, A., de Vos, J., Aubert, M., Kinsley, L., Grün, R., 2013. U-series and radiocarbon analyses of human and faunal remains from Wajak, Indonesia. J. Hum. Evol. 64, 356–365.

Theden-Ringl, F., Hislop, K.P., Aplin, K., Grün, R., Schurr, M.R., 2018. The chronology and environmental context of a cave deposit and associated faunal assemblage including megafauna teeth near Wee Jasper, southeastern Australia. The Holocene 28, 1–16.

Tong, H.W., Guérin, C., 2009. Early Pleistocene *Dicerorhinus sumatrensis* remains from the Liucheng Gigantopithecus Cave, Guangxi, China. Geobios 42, 525–539.

Waterbolk, H.T., 1971. Working with radiocarbon dates. Proc. Prehist. Soc 37, 15–33.

Wood, R., de Quirós, F.B., Maíllo-Fernández, J.M., Tejero, J.M., Neira, A., Higham, T., 2018. El Castillo (Cantabria, northern Iberia) and the transitional Aurignacian: using radiocarbon dating to assess site taphonomy. Quat. Int. 474, 56–70.

Wu, X., Liu, W., Gao, X., Yin, G., 2006. Huanglong Cave, a new late Pleistocene hominid site in Hubei Province, China. Chin. Sci. Bull. 51, 2493–2499.

Yokoyama, Y., Falguères, C., Sémah, F., Jacob, T., Grün, R., 2008. Gamma-ray spectrometric dating of late *Homo erectus* skulls from Ngandong and Sambungmacan, Central Java, Indonesia. J. Hum. Evol. 55, 274–277.

Zhang, X., Zheng, L., Yang, L., Bao, Z., 1991. Human fossils and the paleoculture from Mengzi. In: Museum, Y.P. (Ed.), On Materials of Human Origin and Prehistoric Culture of Yunnan. Yunnan Renming Press, Kunming, pp. 234–246.

Zhao, J., Yu, K., Feng, Y., 2009. High-precision ^{238}U-^{234}U-^{230}Th disequilibrium dating of the recent past–a review. Quat. Geochronol. 4, 423–433.